Influence of collagen fibre orientation on the frictional properties of articular cartilage

Yarimitsu, Seido
Graduate School of Systems Design, Tokyo Metropolitan University

Ito, Kei
Graduate School of Systems Design, Tokyo Metropolitan University

Fujie, Hiromichi
Graduate School of Systems Design, Tokyo Metropolitan University

出版情報：Biosurface and Biotribology. 7 (2), pp.90-97, 2021-05-05. Wiley
バージョン：

Received: 2 October 2020 | Revised: 26 March 2021 | Accepted: 7 April 2021

DOI: 10.1049/bsb2.12005

Biosurface and Biotribology

The Institution of Engineering and Technology WILEY

ORIGINAL RESEARCH PAPER

Influence of collagen fibre orientation on the frictional properties of articular cartilage

Seido Yarimitsu | **Kei Ito** | **Hiromichi Fujie**

Graduate School of Systems Design, Tokyo Metropolitan University, Hachioji, Tokyo, Japan

Correspondence

Seido Yarimitsu, Graduate School of Systems Design, Tokyo Metropolitan University, Hachioji, Tokyo 192-0397, Japan.
Email: yarimitsu@tmu.ac.jp

Funding information

JSPS KAKENHI, Grant/Award Number: JP16H03172

Abstract

Articular cartilage has a unique collagen fibre network structure that exhibits both anisotropy and depth dependency. Collagen fibre orientation in a cross-section parallel to the articular cartilage surface may affect the lubrication properties of articular cartilage. The effect of collagen fibre orientation on the frictional properties of articular cartilage was examined through finite element analysis of the friction. Specifically, a three-dimensional fibre-reinforced poroelastic biphasic model was used to determine the influence of collagen fibril orientation on the frictional properties of articular cartilage. The simulations reveal that collagen fibre orientation has a significant influence on the deformation behaviour of articular cartilage in front of and behind the contact area. The coefficient of dynamic friction was lower in the direction parallel to the collagen fibre orientation than in the direction perpendicular to the collagen fibre orientation, regardless of the indenter speed.

1 | INTRODUCTION

Articular cartilage is an excellent bearing material for synovial joints because it provides extremely low friction and long durability, facilitating various daily activities. Many lubrication theories, including hydrodynamic [1, 2], elastohydrodynamic [1, 3, 4], boundary [5, 6], mixed [1], biphasic [7], and hydration lubrication [8, 9] among others, have been proposed to explain the lubrication mechanism of articular cartilage. These various lubrication mechanisms are expected to function synergistically, depending on the tribological condition in articular joints [10]. This study focused on the importance of biphasic lubrication theory as a key lubrication mechanism of articular cartilage. In biphasic lubrication [11], interstitial fluid, which represents the fluid phase in articular cartilage, supports most of the applied load on cartilage-on-cartilage contact areas, reducing friction [7]. Regarding biphasic lubrication, many experimental and analytical studies have been conducted and the hydraulic permeability of articular cartilage is considered a key factor in the biphasic lubrication mechanism. For example, Reynaud et al. indicated that the hydraulic permeability of articular cartilage is significantly anisotropic under compressive strain [12]. Furthermore, Fujie et al. analysed the effect of anisotropic permeability on the frictional properties of articular cartilage and found that its friction coefficient was improved when the permeability in the cartilage surface layer was set to be 10 times lower in the tangential direction relative to the normal direction [13]. Therefore, the anisotropy of the permeability of articular cartilage is considered important for exhibiting and maintaining the biphasic lubricating function.

Cross-sections perpendicular to the surface reveal that articular cartilage has a complex anisotropic and hierarchical structure [14]. Cartilage layers can be divided into several layers, depending on the orientation of collagen fibres and the morphology of chondrocytes. Collagen fibres are oriented parallel to the surface in the superficial layer, and in the several deeper layers, they are oriented perpendicular to the surface. This unique structure is considered to influence the mechanical properties of articular cartilage. According to a study by Woo et al., the tensile property of cartilage varies dramatically, depending on the relation between the tensile direction and the collagen fibre orientation [15]. In addition, Shirazi et al. reported that collagen fibres oriented perpendicular to the surface in deep layers contribute to increasing the stiffness of cartilage under physiological kinetic conditions [16]. Elsewhere, Hashimoto et al. suggested that the hydraulic permeability of articular cartilage in the normal direction exhibits a depth-dependent decrease together with a depth-dependent increase in the orientation intensity of collagen fibres in the normal direction [17]. Thus, the mechanical properties of

articular cartilage are clearly sensitive to collagen fibre orientation.

We focus on the role of collagen fibres in the superficial layer, which are oriented parallel to the cartilage surface, on the friction-related properties of articular cartilage. The influence of collagen fibre orientation on the frictional properties is examined through an analytical approach using finite element method (FEM) modelling.

2 | METHODS

2.1 | Development of analytical model

We performed the FEM analysis using a poroelastic biphasic model to determine the influence of collagen fibril orientation on the frictional properties of articular cartilage. These cartilage models were developed by considering fibre-reinforced three-dimensional poroelastic elements using Abaqus 2017 (Dassault Systemes, France), as illustrated in Figure 1. The size of the cartilage model was 8.0 × 3.0 × 0.5 mm and composed of poroelastic elements measuring 50 × 50 × 50 μm. The thickness of cartilage model was determined based on the thickness of mature ovine knee cartilage used to obtain the material parameters listed in Table 1. Each element consisted of a pore pressure, a plane strain element (CP3D8RP) representing an anisotropic model of the solid phase of cartilage, and horizontally oriented spring elements (SPRING A) representing the collagen fibres. The material properties of the cartilage model are listed in Table 1. The elastic modus of the solid phase of cartilage was based on our previous study [18]. The Poisson ratio of proteoglycan was obtained from Li et al. [19]. Referring to the method described by Li et al. [20], the elastic modulus of collagen fibres was determined through curve fitting of analytical data to experimental data with polynomial relation obtained from a unidirectional tensile test, in which the tensile direction is parallel or perpendicular to the collagen fibre orientation in a cartilage sample harvested from mature ovine knee cartilage (Figure 2). Thus, the anisotropy of the spring elements in the cartilage model corresponds to the collagen fibril orientation. Based on Equation (1) in the study by Lai et al. [21], permeability k was calculated using the permeability under no strain k_0, permeability coefficients M, and volumetric strain ε. The initial permeability under no strain k_0 in the directions parallel and perpendicular to the collagen fibre orientation was measured in accordance with the method outlined in our previous study [17]. We used a self-made permeability tester and measured k_0 of punched mature ovine cartilage under a confined condition. Permeability coefficients M were determined as the inclination of the permeability-strain logarithmic relation through measuring the strain dependency of the permeability of mature ovine cartilage [22]. Thus, permeability k was calculated as

$$k = k_0 exp(M\varepsilon). \quad (1)$$

where ε represents the volumetric strain of the cartilage matrix.

For the Abaqus calculation, the strain was transformed to porosity ε:

$$\varepsilon = (e - e_0)/(1 + e_0), \quad (2)$$

where e_0 represents the initial porosity, defined as the porosity under no strain. Initial porosity e_0 is defined as V_{p0}/V_{c0}, where V_{p0} and V_{c0} are the initial volume of pore and solid in cartilage matrix, respectively. The water content of articular cartilage is approximately 80% and incompressive interstitial water in cartilage exists at pores in cartilage matrix. Therefore, we defined $V_{p0} = 0.8$ (80%) and $V_{c0} = 0.2$ (20%) and parameter e_0 was set to 4. In subsequent analyses, Equations (1) and (2) were used to determine the permeability of the articular cartilage. The coefficient of friction between the cartilage and the rigid indenter in the solid-to-solid contact region was set as 0.42 in reference to our previous study [23]. The bottom of the model (z-direction) was fixed and impermeable, whereas the sides of the model (x- and y-directions) were unfixed and permeable. The outflow of water from the side and surface of the model was permitted except in the contact region.

2.2 | Friction analysis

Using the articular cartilage model, we performed a friction analysis. A rigid spherical indenter (φ 3.0 mm) was indented to the cartilage surface up to a contact force of 0.1 N, which was maintained for 5.0 s. The indenter was slid over the cartilage surface at sliding speeds of 0.1, 1.0 and 10 mm/s over a sliding distance of 3.0 mm. The temporal change in the coefficient of dynamic friction was calculated from the horizontal force applied to the rigid indenter divided by the contact force. The fluid load support ratio of interstitial fluid pressure α was calculated from the integral of the pore pressure p_w of surface elements in the contact area divided by contact force W using Equation (3):

$$\alpha = \int p_w dS/W, \quad (3)$$

where S represents the contact area between the rigid indenter and cartilage model.

3 | RESULTS

Figure 3 shows the transient of coefficients of dynamic friction acquired in the friction analyses; Figures 4 and 5 summarize the coefficient of friction at start-up and steady state (sliding distance of 2∼3 mm), respectively. The interstitial fluid pressure in the parallel model at a sliding distance of 3 mm is shown in Figure 6. As the sliding speed increases, the interstitial fluid pressure and the fluid load support ratio increase, with the coefficients of start-up and dynamic friction decreasing in both

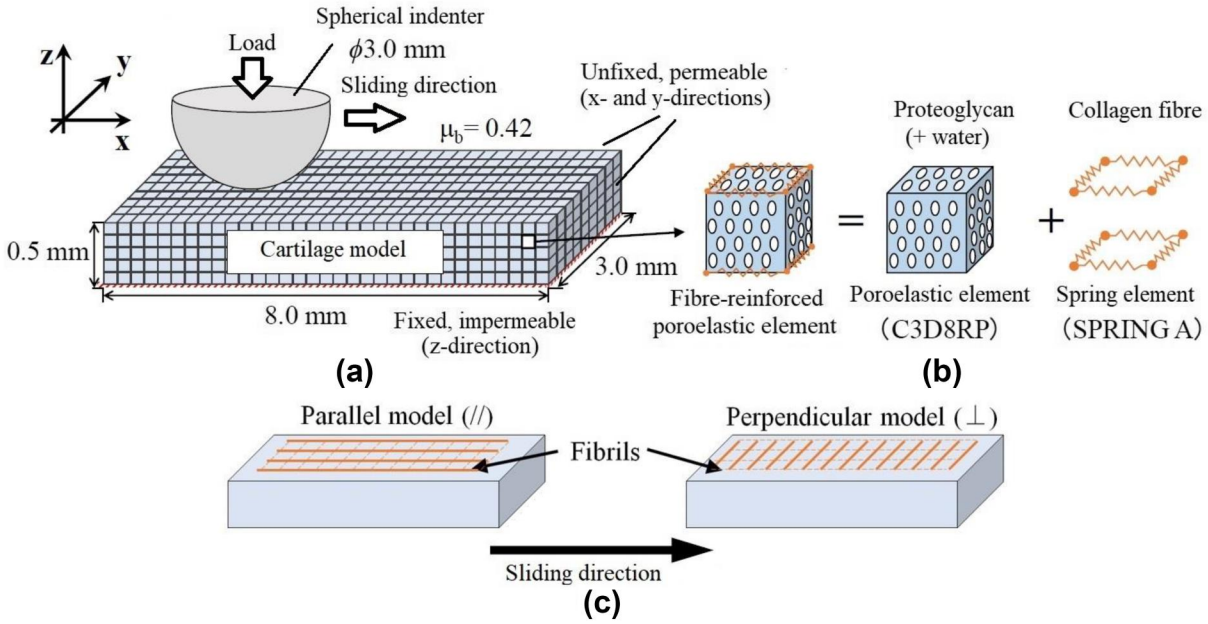

FIGURE 1 Friction analysis for three-dimensional fibre-reinforced poroelastic cartilage model. (a) overview of analysis model; (b) schematics of fibre-reinforced poroelastic element for cartilage model; (c) schematics of fibre orientation in cartilage model

TABLE 1 Mechanical properties of the cartilage model

Solid Phase					Collagen Fibre	
			Permeability [10^{-15} m^4/Ns]			
			$k = k_0 \exp(M\varepsilon)$ [21]			
Model	Modulus [MPa]	Poisson's Ratio	k_0	M	Modulus [MPa] $E_f = E_{f0} + E_{f1}\varepsilon_f$ [19] E_{f0}	E_{f1}
Parallel	0.15 [18]	0.42 [19]	$k_{0x} = 4.05$	$M_x = 10.4$ [22]	$E_{f0x} = 0.2$ $E_{f0y} = 0.08$	$E_{f1x} = 7.0$ $E_{f1y} = 3.5$
			$k_{0y} = 4.35$			
			$k_{0z} = 2.17$ [22]	$M_y = 10.4$ [22]		
Perpendicular			$k_{0x} = 4.35$		$E_{f0x} = 0.08$ $E_{f0y} = 0.2$	$E_{f1x} = 3.5$ $E_{f1y} = 7.0$
			$k_{0y} = 4.05$	$M_z = 9.07$ [22]		
			$k_{0z} = 2.17$ [22]			

Note: k, permeability; k_0, initial permeability under no strain; M, permeability coefficient; ε, volumetric strain of cartilage matrix; E_f, modulus of collagen fibre; E_{f0}, Initial modulus of collagen fibre; E_{f1}, modulus for expressing the strain dependency of fibre modulus; ε_f, tensile strain of collagen fibre.

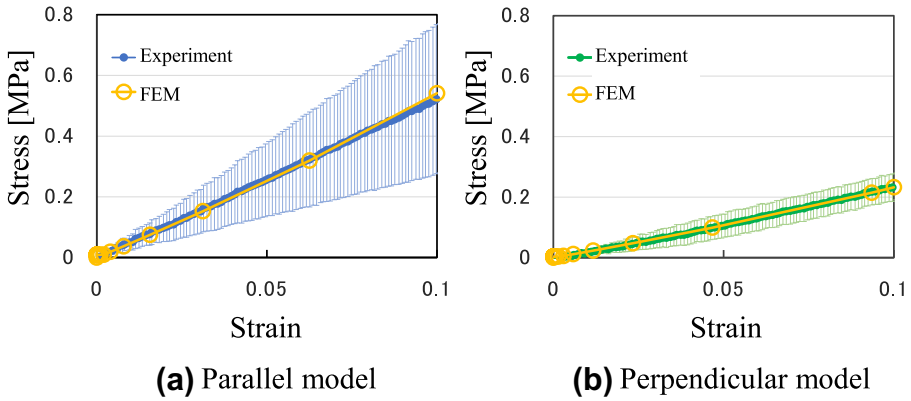

FIGURE 2 Curve fitting of tensile stress to determine the moduli of collagen fibres (experimental data: mean ± standard deviation ($n = 5$)). n, number of samples

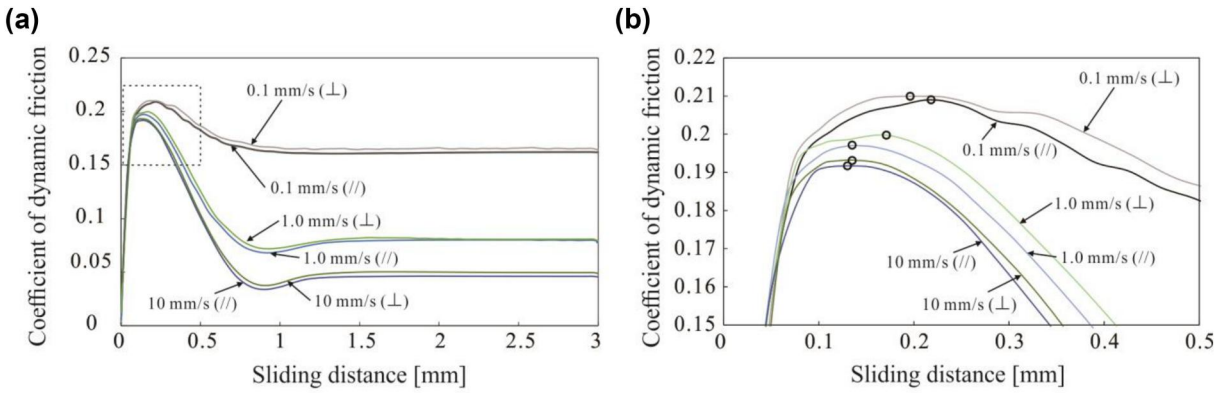

FIGURE 3 Coefficient of dynamic friction in friction analyses. (a) transient of coefficient of dynamic friction; (b) enlarged view of the area surrounded by dotted line in (a) (parallel model://, perpendicular model: ⊥). In (b), plotted circles indicate the maximum points of each curves at start-up motion and the coefficients of dynamic friction at these points are defined as coefficient of start-up friction. Sliding distance at which the coefficients of start-up friction were measured are 0.1 mm/s (//): 0.218 mm, 0.1 mm/s (⊥): 0.196 mm, 1.0 mm/s (//): 0.135 mm, 1.0 mm/s (⊥): 0.171 mm, 10 mm/s (//): 0.130 mm, and 10 mm/s (⊥): 0.135 mm

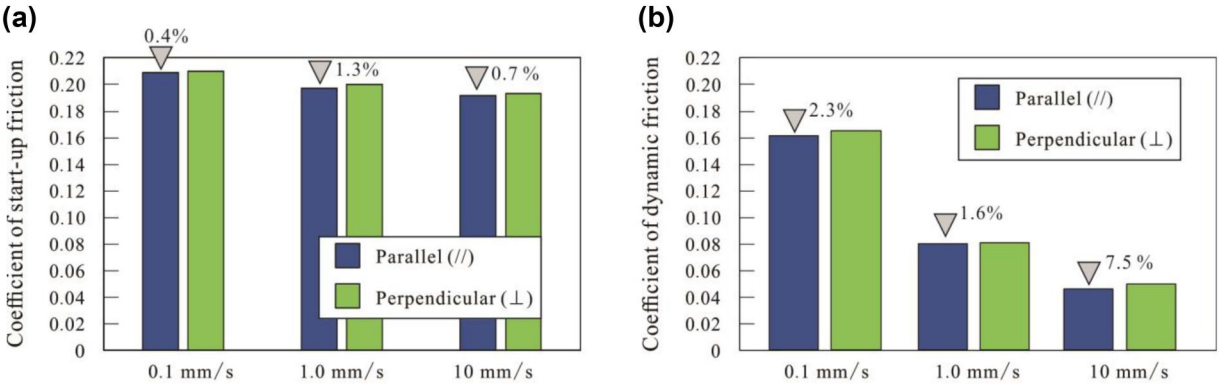

FIGURE 4 (a) coefficient of start-up friction and (b) coefficient of dynamic friction between 2 and 3 mm of the sliding distance. Percentages indicate the decrease in the parallel model relative to the perpendicular model

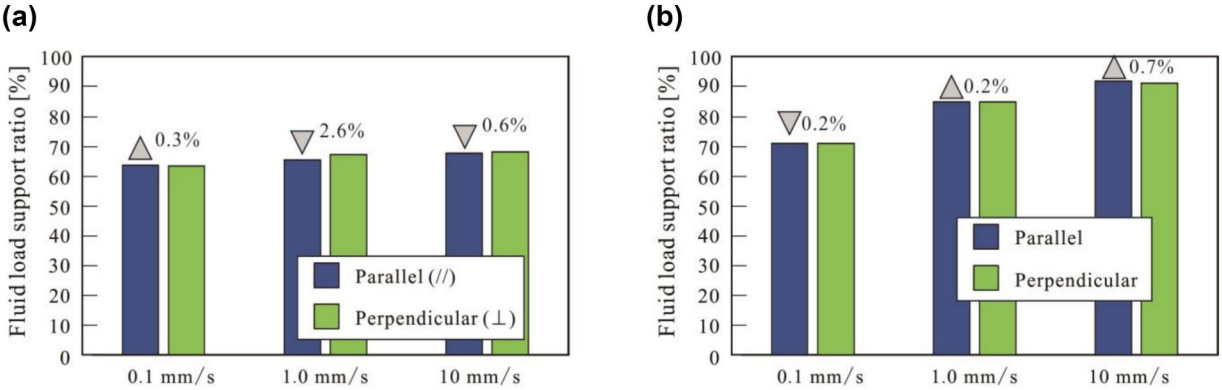

FIGURE 5 Fluid load support ratio of interstitial fluid in cartilage models at (a) start-up friction and (b) steady-state friction. Percentages indicate the increase or decrease for the parallel model relative to the perpendicular model

the parallel and the perpendicular models. In the parallel model, the coefficients of start-up and dynamic friction decreased by up to 1.3% and 7.5% relative to the perpendicular model, respectively (Figure 4). The fluid load support ratio of start-up friction in the parallel model was lower than that in perpendicular model at sliding speeds of 1.0 and 10 mm/s. In

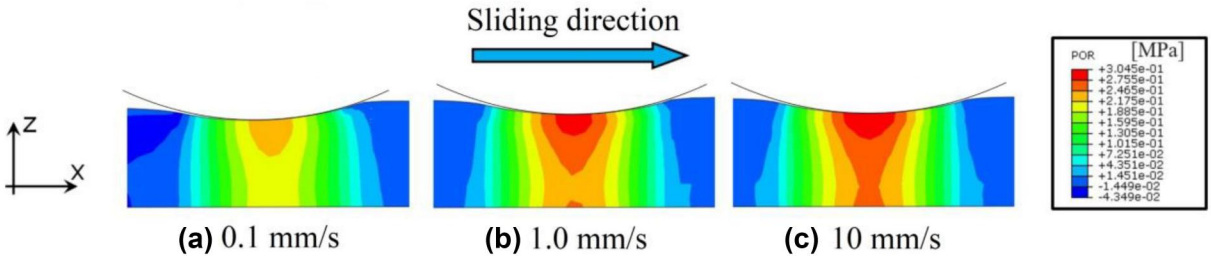

FIGURE 6 Distribution of interstitial fluid pressure in the parallel model at a sliding distance of 3 mm

contrast, this observation was reversed for the steady-state friction, with the parallel model demonstrating a higher ratio at sliding speeds of 1.0 and 10.0 mm/s.

As shown in Figures 7 and 8, the deformation in the parallel model in and in front of the contact area (right side of the indenter in the figures) is lower than for the perpendicular model at start-up friction; this tendency is also observed at steady-state friction. However, the deformation recovery behind the contact area (left side of the indenter in the figures) in the perpendicular model is more noticeable at the lower sliding speeds of 0.1 and 1.0 mm/s.

At start-up friction, the flow rate vectors in front of the contact region are higher in the parallel model than in the perpendicular model for all sliding speed conditions (Figure 9). However, at a sliding distance of 3 mm, the flow rate vectors in front of the contact area in the parallel model are higher than in the perpendicular model under a sliding speed of 0.1 mm/s only (Figure 10).

4 | DISCUSSION

The results of the analysis showed that as the sliding speed increases in both the parallel and perpendicular models, the coefficient of friction decreases whereas the fluid load sharing ratio increases. As shown in Figure 8, the amount of deformation of the models in front of the contact area decreases as the sliding speed increases both for the parallel and the perpendicular models. Consequently, the ploughing friction is reduced. In addition, as the sliding speed increases, the contact region migrates rapidly, leading to less squeezing out of interstitial fluid in the cartilage models. Therefore, interstitial fluid pressure was maintained at a higher level under higher sliding speed conditions (Figure 6), contributing to lowering the friction through the biphasic lubrication mechanism in both the parallel and perpendicular models.

The coefficient of start-up friction in the parallel model is lower than that of the perpendicular model under all sliding speed conditions. Based on the general theory of biphasic lubrication [7], the coefficient of friction is expected to decrease as the fluid load support ratio increases. However, the fluid load support ratio in the parallel model was smaller than that in the perpendicular model under sliding speeds of 1.0 and 10 mm/s. As shown in Figure 9, the outflow of the interstitial fluid was larger in the parallel model than in the perpendicular model under sliding speeds of 1.0 and 10 mm/s. This results in reduced fluid load support in the parallel model. At start-up friction, the deformation in front of the contact area was larger in the perpendicular model than in the parallel model irrespective of sliding speed. Moreover, the friction resistance caused by deformation in front of the contact area in the vertical model is greater than that in the parallel model. Together, these outcomes suggest that the deformation behaviour in front of the contact area may have a greater influence on the frictional behaviour of the cartilage models at start-up friction. The fluid load support ratio in the parallel model at a sliding speed of 0.1 mm/s is slightly higher than that in the perpendicular model despite higher outflow vectors in front of the contact area. This means that the fluid load support ratio of the interstitial fluid at the region closer to the center of the contact area is higher in the parallel model than in the perpendicular model. To clarify the detailed mechanism of this phenomena, the behaviour of interstitial fluid in the contact area must be analysed in more detail using an improved cartilage model with a finer mesh size.

The coefficient of dynamic friction was also lower in the parallel model than in the perpendicular model for all sliding speeds, with the models displaying the greatest difference at a sliding speed of 10.0 mm/s. However, the fluid load support ratio in the parallel model at steady-state friction was lower than in the perpendicular model at a sliding speed of 0.1 mm/s. Deformation just below the indenter and in front of the contact area is remarkably small in the parallel model compared with the perpendicular model. Therefore, deformation resistance during the sliding motion is smaller in the parallel model than in perpendicular model, and this effect is more predominantly responsible for reducing friction of the parallel model at a sliding speed of 0.1 mm/s. The flow rate vectors perpendicular to the model surface were higher in the parallel model than in perpendicular model at a sliding speed of 0.1 mm/s. The reduced deformation in the parallel model relative to the perpendicular model is especially apparent at a sliding speed of 0.1 mm/s; this may be responsible for the suppression of the strain-dependent decrease in permeability in the parallel model, which results in the increased outflow of interstitial fluid at low sliding speeds. Conversely, at sliding speeds of 1.0 and 10 mm/s, the flow rate vectors perpendicular to the model surface are larger in the perpendicular model. As described earlier, the outflow of interstitial fluid from the cartilage model decreases as the speed of contact area

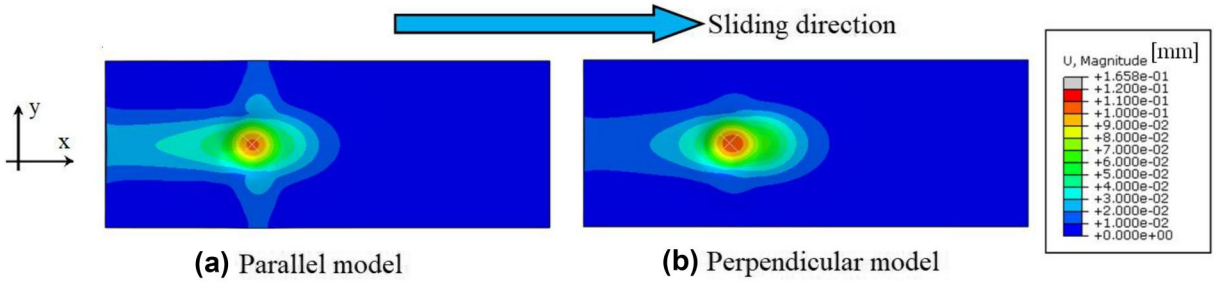

FIGURE 7 Deformation distribution in parallel and perpendicular models at start-up friction (sliding speed of 1.0 mm/s). The magnitude 'U' in the colour bar scale indicates the displacement of the cartilage model

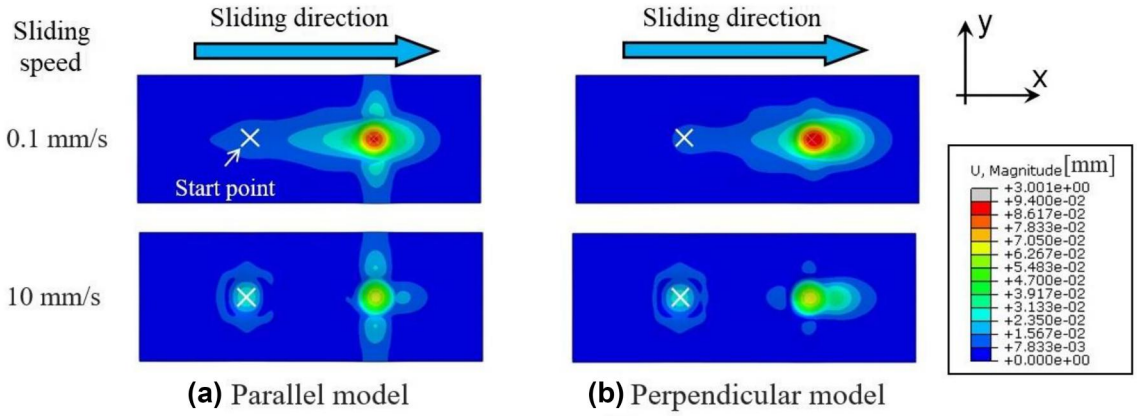

FIGURE 8 Deformation distribution in parallel and perpendicular models at a sliding distance of 3 mm. The magnitude 'U' in the colour bar scale indicates the displacement of the cartilage model

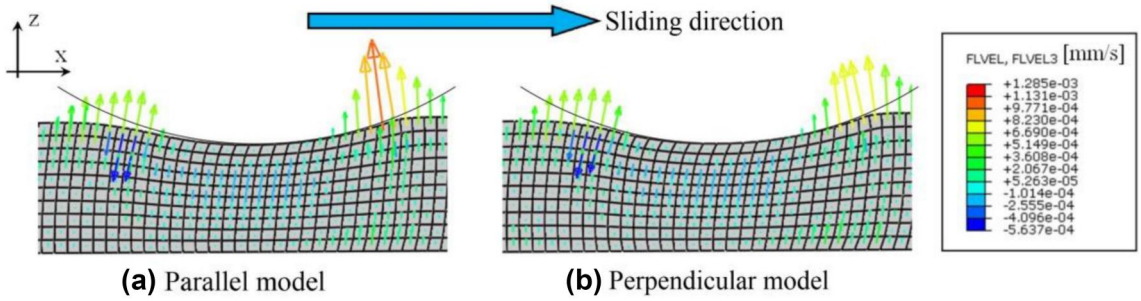

FIGURE 9 Flow rate vectors in the parallel and perpendicular models at start-up friction (sliding speed of 1.0 mm/s)

migration increases. Because the permeability in the direction parallel to the collagen fibres is lower than that in the perpendicular direction, as shown in Table 1, we believe that the outflow of interstitial fluid in front of the contact area is smaller for the parallel model than for the perpendicular model. The parallel model demonstrates lower friction under low sliding speed conditions principally owing to the difference in the extent of deformation within the cartilage model, whereas the parallel model exhibits lower friction under higher sliding speeds because of the difference in the outflow of interstitial fluid and the extent of deformation in front of the contact area.

The difference in friction coefficient between parallel and perpendicular models was small, as shown in Figure 4. Conversely, the analytical results revealed a remarkable difference in the deformation backward the contact area between the models (Figures 7 and 8). Fujie et al. indicated that the deformation recovery backward the contact area influenced the rehydration behaviour of cartilage in a two-dimensional analytical model [24]. The difference in the deformation backward the contact area influences interstitial fluid flow, which in turn may change the frictional behaviour of our cartilage models under a reciprocating sliding condition. We conducted only one-path friction analysis, so the influence of

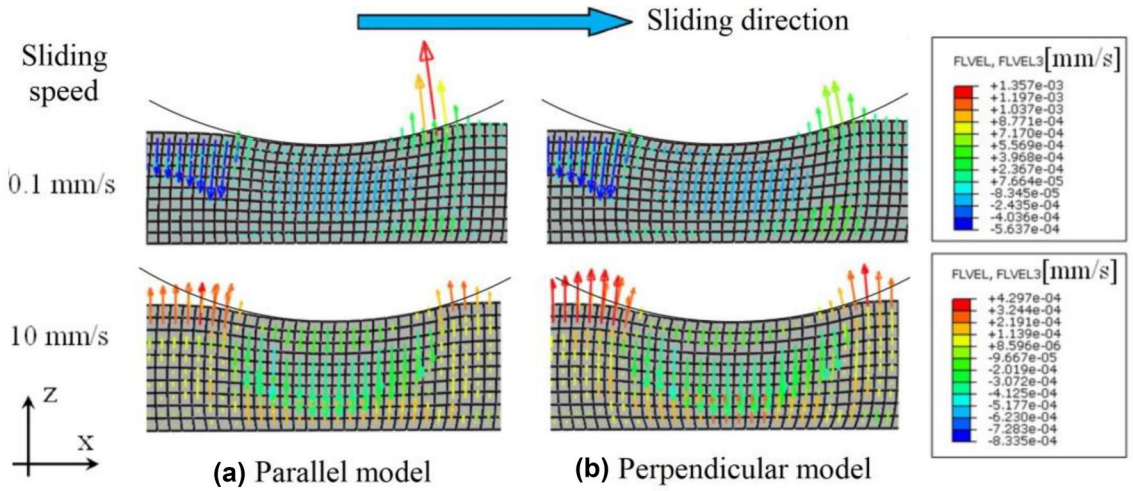

FIGURE 10 Flow rate vectors in parallel and perpendicular models at a sliding distance of 3 mm

deformation recovery on the friction property of articular cartilage must be discussed in future work.

Some additional limitations should be noted. The collagen fibres parallel to the cartilage surface were set in all layers of the cartilage models. However, in articular cartilage, the fibres are oriented parallel to the surface only in the superficial layer, and in the deeper layers they are oriented perpendicular to the surface [14]. Shirazi et al. reported that collagen fibres oriented perpendicular to the surface in the deep layer contribute to increasing the stiffness of cartilage [16]. This suggests that fibres oriented perpendicular to the surface may change the deformation behaviour of cartilage during friction, which may affect the strain-dependent permeability and ploughing friction effect. Therefore, to investigate the effect of collagen fibre orientation on the friction property of articular cartilage in more detail, it is necessary to use a model with a structure closer to the actual fibre orientation structure.

5 | CONCLUSION

We performed FEM analysis using a three-dimensional fibre-reinforced poroelastic biphasic model to determine the influence of collagen fibril orientation on the frictional properties of articular cartilage. Our results revealed that collagen fibre orientation highly influences the deformation behaviour of articular cartilage. The coefficient of dynamic friction was lower in the direction parallel to the collagen fibre orientation than in the direction perpendicular to the collagen fibre orientation, regardless of the sliding speed. These results indicate that collagen fibre orientation is an important factor influencing the frictional behaviour of articular cartilage.

ACKNOWLEDGEMENT

This work was supported by JSPS KAKENHI Grant No. JP16H03172.

ORCID

Seido Yarimitsu https://orcid.org/0000-0002-3923-5769

REFERENCES

1. Dowson, D.: Modes of lubrication in human joints. Proc. IMechE Part 3J. 181, 45–54 (1967)
2. Unsworth, A.: Tribology of human and artificial joints. Proc Inst Mech Eng H. 205, 163–172 (1991)
3. Dintenfass, L.: Lubrication in synovial joints. J Bone Joint Surg. 45(6), 1241–1256 (1963)
4. Dowson, D., Jin, Z.M.: Micro-elastohydrodynamic lubrication of synovial joints. Eng Med. 15(2), 63–65 (1986)
5. Swann, D.A., Radin, E.L.: The Molecular Basis of articular lubrication. J Biol Chem. 247, 8069–8073 (1972)
6. Hills, B.A., Butler, B.D.: Surfactants identified in synovial fluid and their ability to act as boundary lubricants. Ann Rheum Dis. 43, 641–648 (1984)
7. Ateshian, G.A., Wang, H., Lai, W.M.: The role of interstitial fluid pressurization and surface porosities on the boundary friction of articular cartilage. J Tribol. 120, 241–248 (1998)
8. Sasada, T.: Surface gel hydration lubrication in animal joints. J Jpn Soc Tribol. 52(8), 573–578 (in Japanese) (2007)
9. Seror, J., et al.: Supramolecular synergy in the boundary lubrication of synovial joints. Nat Commun. 6, 6497 (2015)
10. Murakami, T., et al.: Adaptive multimode lubrication in natural synovial joints and artificial joints. Proc Inst Mech Eng H. 212(1), 23–35 (1998)
11. Mow, V.C., et al.: Biphasic Creep and stress Relaxation of articular cartilage in compression: theory and Experiments. J Biomech Eng. 102, 73–84 (1980)
12. Reynaud, B., Quinn, T.M.: Anisotropic hydraulic permeability in compressed articular cartilage. J Biomech. 39, 131–137 (2006)
13. Fujie, H., Imade, K.: Effect of low tangential permeability in the superficial layer on the frictional property of articular cartilage. Biosurf. Biotribol. 1(2), 124–129 (2-15)
14. Pearle, A.D., Warren, R.F., Rodeo, S.A.: Basic science of articular cartilage and osteoarthritis. Clin Sports Med. 24, 1–12 (2005)
15. Woo, S.L.Y., et al.: Large deformation nonhomogeneous and directional properties of articular cartilage in uniaxial tension. J Biomech. 12, 437–446 (1979)
16. Shirazi, R., Shirazi-Adl, A.: Deep vertical collagen fibrils play a significant role in mechanics of articular cartilage. J Orthop Res. 26, 608–615 (2007)
17. Hashimoto, N., et al.: Depth dependency of hydraulic permeability of articular cartilage. Jap. J. Clin. Biomech. 38, 7–12 (in Japanese) (2017)

18. Hashimoto, N., et al.: Effect of maturation on the hydraulic permeability of articular cartilage. Jap. J. Clin. Biomech. 39, 293–298 (in Japanese) (2018)
19. Li, L.P., et al.: Nonlinear analysis of cartilage in unconfined ramp compression using a fibril reinforced poroelastic model. Clin BioMech. 14, 673–682 (1999)
20. Li, L.P., Cheung, J.T.M., Herzog, W.: Three-dimensional fibril-reinforced finite element model of articular cartilage. Med Biol Eng Comput. 47, 607–615 (2009)
21. Lai, W.M., Mow, V.C.: Drag-induced compression of articular cartilage during a permeation experiment. Biorheology. 17(1-2), 111–123 (1980)
22. Hashimoto, N.: report Effects of the hydraulic permeability of articular cartilage on the lubrication property. Master Thesis, Tokyo Metropolitan University Hino, Tokyo (in Japanese) (2018)
23. Imade, K., et al.: Effects of interstitial fluid and boundary condition on the start-up friction behaviour of cartilage. In: Proceedings of. International. Conference on Biotribology. Xi'an. 34 (2012)
24. Fujie, H., Morishita, S., Yarimitsu, S.: Effect of collagen-induced residual stress on the frictional property of articular cartilage. Biosurface and Biotribology. 4(2), 68–71 (2018)

How to cite this article: Yarimitsu S, Ito K, Fujie H. Influence of collagen fibre orientation on the frictional properties of articular cartilage. *Biosurface and Biotribology*. 2021;7:90–97. https://doi.org/10.1049/bsb2.12005